USE OF LAB CONSTRUCTED NITROGEN LASER FOR RAMAN AND LASER–INDUCED FLUORESCENCE SPECTROSCOPY STUDIES

By

Tesfaye Mamo

SUBMITTED IN PARTIAL FULFILLMENT OF THE
REQUIREMENTS FOR THE DEGREE OF
MASTER OF SCIENCE
AT
ADDIS ABABA UNIVERSITY
ADDIS ABABA, ETHIOPIA
JUNE 2020

© Copyright by Tesfaye Mamo, 2020

ADDIS ABABA UNIVERSITY
DEPARTMENT OF
PHYSICS

The undersigned hereby certify that they have read and recommend to the Faculty of Science for acceptance a thesis entitled "**USE OF LAB CONSTRUCTED NITROGEN LASER FOR RAMAN AND LASER–INDUCED FLUORESCENCE SPECTROSCOPY STUDIES**" by **Tesfaye Mamo** in partial fulfillment of the requirements for the degree of **Master of Science**.

Dated: June 2020

Supervisor: _____
Prof. A.V. Gholap

Examiners: _____
Dr. Abebe Belay

_____
Dr. Alemu Kebede

ADDIS ABABA UNIVERSITY

Date: **June 2020**

Author: **Tesfaye Mamo**

Title: **USE OF LAB CONSTRUCTED NITROGEN LASER FOR RAMAN AND LASER–INDUCED FLUORESCENCE SPECTROSCOPY STUDIES**

Department: **Physics**

Degree: **M.Sc.** Convocation: **June** Year: **2020**

Permission is herewith granted to Addis Ababa University to circulate and to have copied for non-commercial purposes, at its discretion, the above title upon the request of individuals or institutions.

Signature of Author

THE AUTHOR RESERVES OTHER PUBLICATION RIGHTS, AND NEITHER THE THESIS NOR EXTENSIVE EXTRACTS FROM IT MAY BE PRINTED OR OTHERWISE REPRODUCED WITHOUT THE AUTHOR'S WRITTEN PERMISSION.

THE AUTHOR ATTESTS THAT PERMISSION HAS BEEN OBTAINED FOR THE USE OF ANY COPYRIGHTED MATERIAL APPEARING IN THIS THESIS (OTHER THAN BRIEF EXCERPTS REQUIRING ONLY PROPER ACKNOWLEDGEMENT IN SCHOLARLY WRITING) AND THAT ALL SUCH USE IS CLEARLY ACKNOWLEDGED.

to my Parents and Family

Table of Contents

List of Tables

List of Figures

Abstract

In this work we have constructed a functioning Nitrogen lasers with different electrode materials and different sized aluminum foil capacitors with success. With the result we went ahead with the Raman spectroscopic study of polystyrene sample, which is used as food packaging material and as insulator in transportation of fragile materials, and acquired the standard spectra of polystyrene found in reference spectral database with a close Raman shift of Raman peak values. We also pumped Rhodamine 6G dye successfully and used the dye laser for the fluorescence spectroscopic study of edible niger seed oil. We have seen that there is a linear relationship of contamination of the pure niger seed oil with that of heated niger seed oil simulating a used oil in cooking food. We have been able to detect a minimum of 1.61% contamination and show that there might be a new fluorophores formation due to the heating of the oil.

Acknowledgments

I am very grateful to my advisor Prof. A.V. Gholap, who shared his unreserved and vast knowledge and passion of working with the nitrogen lasers.

To my lovely wife, Hiwot Kassa, I thank you so much for giving me time to work on this paper while taking care of our children and understanding my silence while I am thinking of the work.

I would also like to thank the Physics department and Addis Ababa University for the support and allowing me to study my MSc.

I am thankful for Dr. Araya Asfaw and Dr. Mesfin Redi for their support and encouragement.

For material support I thank the chemistry department with their unreserved supply of laser dyes and especially Prof. Wondmagegn Mammo for using their dewar and frequent fill of liquid nitrogen.

Tesfaye Mamo

June 27, 2020.

Abbreviations

C1	Capacitor 1
C2	Capacitor 2
CARS	Coherent Anti-Stokes Raman Scattering
CW	Continuous Wave
DPSS	Diode Pumped Solid State
DVD	Digital Video Disc
IR	Infra Red
KHD	Kramer-Heisenberg-Dirac
KV	Kilo Volt
KW	Kilo Watt
LIDAR	Light Detection and Ranging
MW	Mega Watt
ND:YAG	Neodymium Yttrium Aluminum Garnet
nm	nano meter
ns	nano second
OPA	Optical Parametric Amplifier
OPO	Optical Parametric Oscillator
pF	pico Farad
QCW	Quasi-Continuous Wave
RRS	Resonance Raman Scattering
SERRS	Surface Enhanced Resonance Raman Scattering
SERS	Surface Enhanced Raman Scattering

SFM	Shear Force Microscopy
SG	Spark Gap
SPM	Scanning Probe Microscopy
STM	Scanning Tunneling Microscopy
SW1	Switch 1
SW2	Switch 2
SW3	Switch 3
TEA	Transversely Excited at Atmospheric pressure
TERS	Tip Enhanced Raman Scattering
UV	Ultra Violet
W	Watt

Chapter 1

Introduction

1.1 Basic concept of Lasers

Laser is an acronym for Light Amplification by Stimulated Emission of Radiation. This means a laser generates and/or amplifies light energy. Unlike a black body emission such as incandescent light bulb, lasers generate light of a very sharp spectral line, directional and coherent beam of light. These properties of lasers make them very useful in most researches which use light. Apart from their use in laboratories, lasers are embedded in our everyday use.

From small power lasers in DVD and Blueray players in our homes, supermarket bar code scanners, to medium to high power medical lasers for eye surgery or safe surgery for diabetic patients and Peta-Watt power lasers in nuclear fusion facilities, the role of lasers is paramount.

The special properties of laser light described above led to very diverse areas of studies and applications in physics, chemistry, biology, material science, telecom etc. Nowadays it is hard not to find lasers in use in our daily life. These days lasers are used, in its one area of application, as LIDARs in modern cars for collision avoidance method for autonomous driving.

Lasers can be categorized based on:

- Pumping mechanism
  - Optically pumped lasers
  - Electrically pumped lasers
  - Chemically pumped lasers
- Mode of operation
  - Continuous Wave lasers(CW)
  - Quasi-Continuous Wave lasers(QCW)
  - Pulsed lasers
- Lasing medium
  - Gas lasers
  - Solid state lasers
  - Semiconductor lasers
  - Liquid, Dye and Chemical lasers.

Nitrogen laser is a very useful laser in spectroscopic studies by using it by its own or pumping dyes to give a highly tunable laser source which was not possible by other types of lasers. For example, the common HeNe laser only gives a 632.8 nm red laser. Even if a HeNe laser can operate on other wavelengths such as 543.3 nm (Green), 594.0 nm (yellow), 612.0 nm (orange), and also the common 632.8 nm (red) in the visible spectrum and 1150 nm, 1523 nm and 3390nm in the Infra-Red spectrum

and is commercially available, it is not completely (continuously) tunable. Therefore, tunable lasers in form of dye lasers are the most attractive ones because of their simplicity. Although tunable lasers spanning from UV to IR range are possible using DPSS (Diode Pumped Solid State) lasers with OPO (Optical Parametric Oscillator) and OPA (Optical Parametric Amplifier) lasers, they are currently very expensive. Pumping of dye lasers with nitrogen laser is the most commonly used set up in laboratories with out high financial capacity such us ours.

Another advantage of the nitrogen laser is its pulsed nature, with duration in order of sub-nanosecond at atmospheric pressure to tens of nanoseconds at low pressures, which avoids triplet states of dye lasers.

This can be seen by the fact that no dye re-circulation is needed while being pumped by nitrogen lasers but rather only shaking of the cuvette with a vibrator to agitate the dye is necessary. Its rectangular shape can be focused using a cylindrical lenses to a narrow line shaped beam profile so that it can be used to pump dyes in a cuvette. However, in case of using CW lasers for pumping of the dyes, we have to use recirculating dye with dye reservoir and a pump to make a flowing jet of the dye across the beam path of the pumping lasers such as Argon ion at 514.5 nm or second harmonic of Nd:YAG at 532 nm.

In this work, we will use a electrically pumped, pulsed and a nitrogen gas medium laser that is constructed here in our laboratory for spectroscopy works of Raman and fluorescence study of selected samples. We also used it as dye pumping UV source. The advantage of the supperradiant nature of the nitrogen laser is there is no need of optical cavity forming mirrors. Unlike most lasers, there is no need of expensive and unavailable noble gas such as helium, neon or vacuum pump. The only material we

had to buy was aluminum foil from local market. Other items are already available in our laboratory or some are extracted from old PC monitors.

1.2 Objective

In this work we are trying to:

- Construct a functional nitrogen TEA lasers and pump dye lasers.
- Use the constructed laser as excitation source for a Raman spectroscopy study of polystyrene polymer sample.
- Study laser-induced fluorescence of heated niger seed oil for adulteration of edible oils.

1.3 Specific Objectives

We try to maximize the laser output power as best as we can by changing electrode type and size. In the Raman experiment, we selected a sample with no absorbance at the laser frequency and avoid fluorescence of the sample. With respect to the fluorescence we made effort in the sample preparation to get smallest detectable variation in concentration of adulterated edible oil.

1.4 Outline

Chapter one, here, gave the overall introduction and objective of the work. Chapter two introduces the theoretical basis of nitrogen gas lasers, Raman spectroscopy, types of Raman spectroscopy and fluorescence spectroscopy.

In chapter three, experimental setup, the nature of the samples and instrumentation of the spectroscopy studies are described. Calibration procedures are also presented.

Chapter four will contain the results, analysis and discussion of these three experiments. Here, comparisons with other works and references are given.

Chapter five will give the conclusions of our work and the recommendation, and also future prospects of these experiments are proposed.

In the next chapter we will see the theoretical background of the nitrogen lasers, Raman spectroscopy and laser-induced fluorescence spectroscopy.

Chapter 2

Theory

2.1 Nitrogen Lasers

Pumping of nitrogen molecules as a source of ultra violet coherent light of wavelength 337.1 nm, with high intensity and other dozens different lines at a wavelength range of 300 nm to 400 nm with duration of about 20 ns due to the emission from the second positive group, $C^3\pi_u \rightarrow B^3\pi_g$ using 100–150 KV and plasma tube of length 48 inches (121.92 cm) with peak out put power of 10 W was first shown in the work of H.G. Heard [13]. Later Leonard [18] and Gerry [10] used transverse excitation of the nitrogen laser and produced a power of 200 KW using 128 segmented electrodes contained in a 2 meters long channel. The segmented electrodes were connected by coaxial cables through a triggered spark gap to a capacitor. The setup used by Leonard is shown in Fig 2.1. Shipman[28], using Blumlein pulse generator of flat-plate transmission line of size 183 cm wide and 366 cm long, produced a 2.5 MW peak power laser pulse with duration of 4 ns. A charging voltage of around 75KV and 1.5 mm thick mylar dielectric were used in this setup. A traveling excitation wave was generated by the firing of the solid dielectric switches sequentially at precise interval by carefully prepared coaxial trigger cables and he achieved electromagnetic wave in

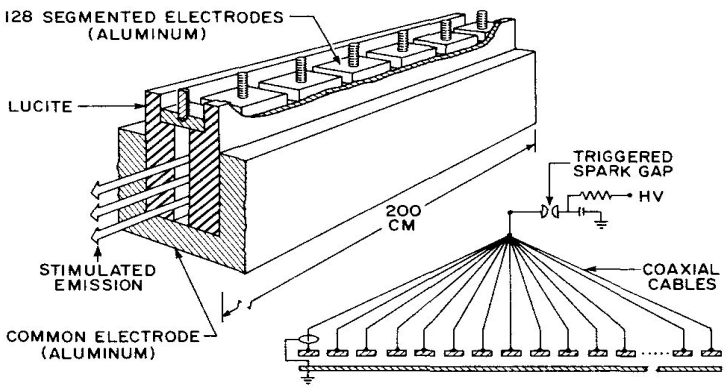

Figure 2.1: Setup of nitrogen laser in the work of Leonard with 128 segmented electrodes.

the Blumlein line crossing the discharge tube at an angle so that the excitation current wave traveled down the laser channel with a phase velocity equal to the velocity of light[28]. Patel[22] used trapezoidal plate as one of the top plates of the capacitor in a modified Blumlein configuration, and the other side of the cavity was made of 5 plates facing the trapezoidal plate to form the laser channel. With total capacitance of 2200 pF and a charging voltage of 30 KV, he was able to produce close to 1 MW pulse with a duration of about 0.6 ns while Basting *et al.*[7] produced 1.2 MW peak power using 30 cm active length and a helium-nitrogen mix at 20 KV at 1 atm.
The highest peak power and efficiency of nitrogen lasers is produced by Godard with 9 MW peak power and 1% efficiency[11].

2.1.1 Working Principle of Nitrogen Lasers

Populating of the level $C^3\pi_u$ of Nitrogen molecule in short time with respect to the natural radiative lifetime of 40 ns, it will be possible to establish population inversion between $C^3\pi_u$ and $B^3\pi_g$ levels of the second positive system of the nitrogen molecule to obtain stimulated emission. The $B^3\pi_g$ level has a lifetime of 5-8 μs [11].

The life time of τ of the upper laser level at a pressure p(torr) is given by[32]:

$$\tau(ns) = \frac{36}{1 + \frac{p}{58}} \tag{2.1.1}$$

which shows at atmospheric pressure of 760 torr, the life time will be 2.55 ns. According to Ali *et al.*[3], we can consider the 337.1 nm emission of the nitrogen laser as a three-level laser with $X^1\Sigma_g^+$ (ground-state level) $B^3\pi_g$ (low-level 2) and $C^3\pi_u$ (high-level 3) as shown in Fig 2.2.

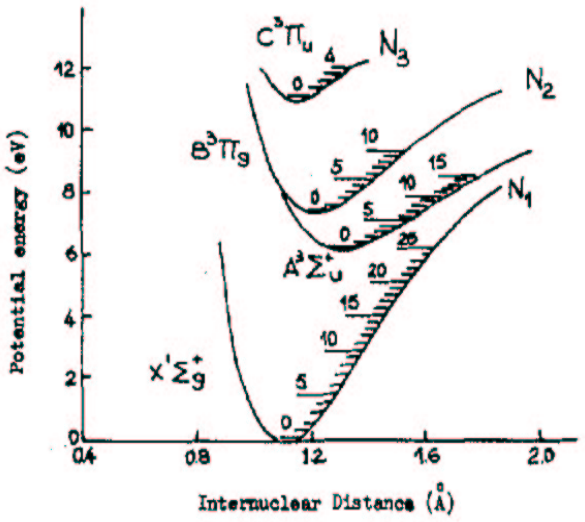

Figure 2.2: Energy level diagram of nitrogen molecule in nitrogen laser[11]

Let N_1, N_2 and N_3 represent the population densities of the ground state, lower state and upper laser levels of the nitrogen laser respectively. Let X_{ij} be the rate of excitation by collision by electron impact from level i to j with $i < j$ and Y_{ji} to represent the rate of collisional deexcitation from j to i and τ_{ji}^{-1} be the rate of radiative decay from j to i and let R_{ji}^i be the rate of induced emission which includes the line width, Einstein's B coefficient, and the energy density[3].

The rate equations for the three levels can be written as:

$$\frac{dN_3}{dt} = X_{13}N_1 + X_{23}N_2 - (Y_{31} + Y_{32} + \tau_{32}^{-1})N_3 - R_{32}^i[N_3 - (g_3/g_2)N_2] \tag{2.1.2}$$

$$\frac{dN_2}{dt} = X_{12}N_1 + (Y_{32} + \tau_{32}^{-1})N_3 - (\tau_{21}^{-1} + Y_{21} + X_{23})N_2 + R_{32}^i[N_3 - (g_3/g_2)N_2] \tag{2.1.3}$$

$$\frac{dN_1}{dt} = -(X_{12} + X_{13})N_1 + (Y_{21} + \tau_{21}^{-1})N_2 + (\tau_{31}^{-1} + Y_{31})N_3 \tag{2.1.4}$$

Where g_3 and g_2 are the statistical weights of upper and lower laser levels, respectively. Analytically solved under certain assumptions, general criteria in the steady state and pulsed laser action are obtained[3]. For demonstration of the collisional effect of the laser levels by electron impacts the above equations are applied to the nitrogen molecule electronic transition $C^3\pi_u(\nu = 0) \rightarrow (\nu = 0)$ at 337.1 nm is considered. As mentioned above N_3, N_2 and N_1 are the population densities of $C^3\pi_u$, $B^3\pi_g$ and the ground state of the nitrogen molecules, respectively. Here induced emission, absorption rates and deexcitation from the laser levels to the ground state are neglected. Using the fact that $\tau_{31}^{-1} \gg \tau_{32}^{-1}$(because the C state is metastable) and $X_{13} > X_{12}$ according to Frank-Condon principle which states that transitions are more favorable from states with close proximity of nuclear coordinates, and $\tau_{21} \gg \tau_{32}$ ($\tau_{32} \simeq 40ns$ and $\tau_{21} \simeq 10\mu s$) we can write the sum of Eq 2.1.2 and Eq 2.1.3 as

$$\frac{d(N_1 + N_2)}{dt} = X_{13}N_1 \tag{2.1.5}$$

and get the following equation by integrating Eq 2.1.5 by assuming N_1 and the pumping rate are constants.

$$(N_1 + N_2) = X_{13}N_1 t \tag{2.1.6}$$

By using Eq 2.1.6 and Eq 2.1.2 with the above assumption, we get

$$\frac{dN_3}{dt} = X_{13}N_1 + [X_{13}N_1 - N_3]X_{13} - \beta N_3 \tag{2.1.7}$$

where $\beta = (\tau_{32}^{-1} + Y_{32})$. Integration of Eq 2.1.7 results in

$$N_3 = (X_{13}N_1/\alpha^2)(Y_{32} + \tau_{32}^{-1}) - (X_{13}N_1/\alpha^2)(e^{-\alpha t}) + (N_1 X_{13} X_{23} t/\alpha) \tag{2.1.8}$$

where $\alpha = \beta + X_{23}$.

For small value of t, we can write Eq 2.1.8 after expanding the $e^{-\alpha t}$ as

$$N_3 = X_{13}N_1 t - \frac{1}{2}X_{13}N_1(Y_{32} + \tau_{32}^{-1})t^2 \tag{2.1.9}$$

Combining Eq 2.1.6 and Eq 2.1.9 we get

$$N_2 = \frac{1}{2}X_{13}N_1(Y_{32} + \tau_{32}^{-1})t^2 \tag{2.1.10}$$

To get population inversion, i.e., $N_3 > N_2$ we can see that from Eq 2.1.9 and Eq 2.1.10 we have to have the condition

$$t < 1/(Y_{32} + \tau_{32}^{-1}) \tag{2.1.11}$$

The relation in Eq 2.1.11 implies that the population inversion can take place in a small time t compared to $(Y_{32} + \tau_{32}^{-1})$

For $\tau_{32}^{-1} > Y_{32}$, Eq 2.1.11 gives Bennett's criterion for inversion in a pulsed laser as [6]:

$$t \lessapprox 1/2A_{32} \tag{2.1.12}$$

where A_{32} is Einstein's A coefficient For laser transition, A_{32} has typical value of (10^7 to 10^8)/s. This need for a very fast excitation to achieve population inversion led to the fast discharge mechanism of the circuits. One of this circuit is the Blumlein type excitation using Blumlein configuration as shown in Fig 2.3. The most efficient of these lasers is about 1% and peak power of 9 MW as presented in the work of Godard[11]. Another rare, and not reproduced to our knowledge, 2.15 MW and 3%

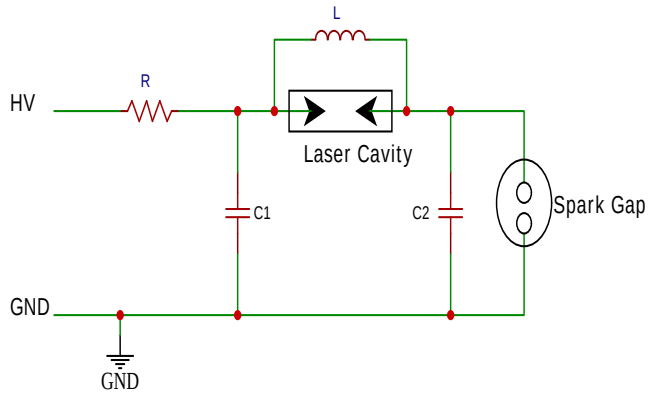

Figure 2.3: Blumlein circuit for nitrogen laser

efficiency is reported in the work of Oliveira *et al.*[5].

What makes nitrogen lasers attractive, even to these days, is the ease of construction and using them on their own as UV laser or as pumping lasers for dye lasers. Which is also the case and motivation in this work. Therefore, it is important to know how a Blumlein circuit functions to produce a nitrogen laser.

As we have seen above, we require fast discharge to achieve population inversion and hence a laser output. The Blumlein with low total inductance is needed since inductance slows down the system and it should be minimized as much as possible.

The lasing process starts with capacitors C1 and C2 being charged with a high voltage source HV. Since the two top plates of the capacitors are connected to each other via a resistor and/or inductor, they will have at this time, the same voltage with the laser channel being in the middle of these capacitors. After a while, when the voltage is high enough and break down voltage is reached at the spark gap, the spark gap conducts shorting out capacitor C2 and swings the voltage to a negative value. At this moment C1 is still charged to the initial voltage and now a massive voltage appears in the laser channel which we put between the two capacitors. Charge from C1 flows to C2 across

the laser channel exciting the nitrogen molecules in the laser channel and produce the 337.1 nm laser[2]. Here if we use the atmosphere which has 78% nitrogen it is called TEA laser. A high percentage of nitrogen gas will naturally give more laser power. A low inductance capacitor made of aluminum or copper, a very thin dielectric capable of withstanding the high voltage and a carefully selected spark gap material helps in reducing the inductance of the laser system. The spark gap can be free running or triggered. The circuit oscillation is depicted in Fig 2.4. Initially switches SW1

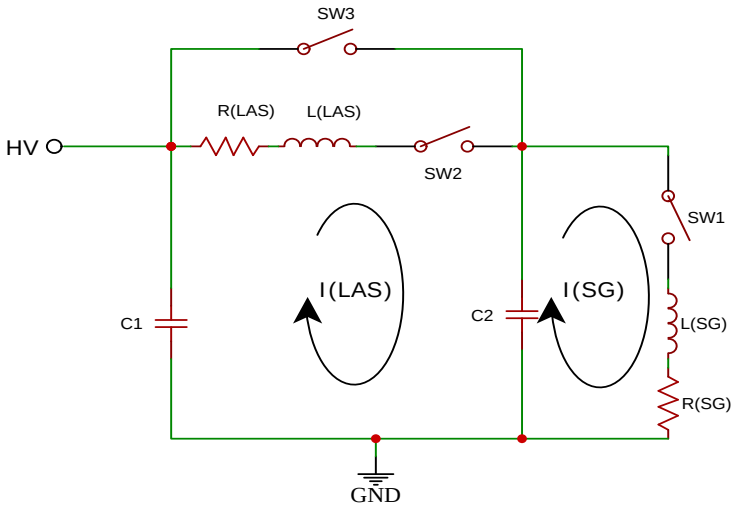

Figure 2.4: Equivalent circuit of Blumlein for charging/discharging [2]

(spark gap) and SW2 (laser channel) are open while SW3 (inductor) is closed acting as a simple conductor. When the spark gap breaks down it becomes conductive and SW1 closes there will be a current I_{SG} through the RLC circuit formed by R_{SG}, L_{SG} and C2 which oscillates with angular frequency $\omega \approx (L_{SG}C2)^{-1/2}$. Now the SW3 switch, being an inductor, have high impedance not allowing current flow opens and the voltage across the laser channel begins to oscillate with the same frequency, rising

from zero to close to 2 times the initial voltage. But before the voltage reaches double of the initial voltage across the laser channel, it closes SW2 since break down of the nitrogen gas occurs and the current I_{LAS} flows in the other loop shown in Fig 2.4[2]. In both atmospheric (considered high pressure) or low pressure operation of the laser, we can use a flowing gas to purge molecules which are in metastable state since only molecules in the ground state can be pumped. Purging of the gas by flowing the fresh high purity nitrogen gas can be done in two ways. The most effective type of purging is shown to be flowing the gas transverse to the electrodes rather than parallel to the electrodes with energy increase factor of two and reduce the pulse width by 2 ns increasing the power more than a factor of two in the work of Saito *et al.*[33]. A consideration for longevity of lab constructed nitrogen lasers is the breakdown of the dielectric. The stress of charging and discharging will ultimately results in failure. One interesting work we have seen by Cubeddu *et al.*.[24] uses distilled water as dielectric. This setup has many advantages since if the dielectric breaks, it is automatically fixed for the next charge because there will not be a permanent physical damage that we see in thin solid dielectric materials such as mylar or transparency sheet. Additional advantage of using water is the fact that water has dielectric constant of $\sim$80 compared to transparency sheet with value of only 2 which is a factor of 40 more capacitance which will allow a smaller size setup.

2.2 Raman Spectroscopy

Interactions of light with matter is the basis of spectroscopic studies of materials. Absorption, emission-after-absorption such as fluorescence and phosphorescence, scattering etc., are examples of light-matter interactions. One of these interaction, scattering, is one important aspect of light-matter interaction. The most common form of scattering is Rayleigh scattering in which the incident light is scattered back with out any change in the wavelength of the incident light. But, even though small, there is another form of scattering with a change in wavelength of the scattered light what we call Raman scattering, bearing the name of the discoverer C. V. Raman, with K. S. Krishnan [27].

When Raman discovered this effect, which we call now Raman effect, he used a 7 inch telescope objective and short focus lens to concentrate the sunlight and filtered it using blue-violet filter to excite the sample and a green glass was used to view the opalescent track with in the sample [27].

This is what we now call the first filter a laser line filter which is used to clean the laser line to a single wavelength and the second filter is Rayleigh rejection filter which suppresses the incident laser line. This arrangement is is used in every modern Raman spetrometers.

Raman effect is the result of inelastic scattering of the incident light from the vibrating molecules. A classical description of Raman scattering is described by the interaction of the incident oscillating electromagnetic field with inducing polarization of the molecule. The induced dipole radiated a scattered light with or without exchanging energy with the vibrating molecule. The strength of the induced polarization μ_{ind} is

proportional to the the polarizability α and the incident electric field E expressed as:

$$\mu_{ind} = \alpha E \tag{2.2.1}$$

And the electric field of the incident light can be written as:

$$E = E_0 cos(2\pi t \nu_0) \tag{2.2.2}$$

where E_0 is the field strength and ν_0 is the frequency of oscillation of incident light. In simple form, the displacement of atoms in molecules can be expressed as:

$$Q = Q_0 cos(2\pi t \nu_{vib}) \tag{2.2.3}$$

where Q_0 is the amplitude of oscillation about equilibrium and ν_{vib} is frequency of vibration.

For small displacements, as in the case here, the polarizability can be approximated by Tyler expansion in normal coordinates as:

$$\alpha = \alpha_0 + (\frac{\partial \alpha}{\partial Q})_0 Q \tag{2.2.4}$$

The subscript 0 indicates both terms are evaluated at the equilibrium position of the atoms. The polarizability has now two terms. The first term is static, and the second term is sinusoidally oscillating. For Raman scattering to occur, the polarizability needs to change with the vibration that is to say $(\frac{\partial \alpha}{\partial Q})_0 \neq 0$. Substituting Equations Eq 2.2.2, Eq 2.2.3 and Eq 2.2.4 in Eq 2.2.1, we get

$$\mu_{ind} = \alpha_0 E_0 cos(2\pi\nu_0 t) + (\frac{\partial \alpha}{\partial Q})_0 \frac{E_0 Q_0}{2} [cos(2\pi(\nu_0 + \nu_{vib})t) + cos(2\pi(\nu_0 - \nu_{vib})t] \tag{2.2.5}$$

With the classical model, we have derived Eq 2.2.6 and it shows that the induced dipole moment emits radiation at ν_0, $\nu_0 + \nu_{vib}$(blue-shifted) and $\nu_0 - \nu_{vib}$(red-shifted).

We know the scattering at these frequencies as Rayleigh, anti-Stokes and Stokes scattering, respectively.

As we can see from Fig 2.5, anti-Stokes Raman intensity will depend on the population of the first vibrationally excited states. This intensity is related to temperature and the ratio of anti-Stokes and Stokes is given by a Boltzmann distribution as:

$$\frac{I_{Anti-Stokes}}{I_{Stokes}} = \frac{(\nu_0 + \nu_{vib})^4}{(\nu_0 - \nu_{vib})^4} \exp(\frac{-h\nu_{vib}}{KT}) \tag{2.2.6}$$

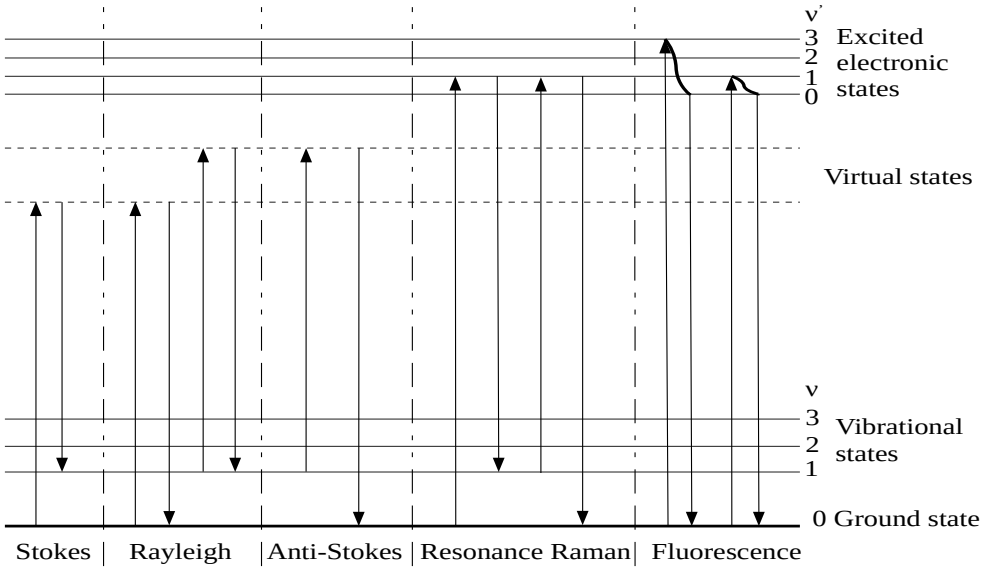

Figure 2.5: Jablonski diagram for Raman and fluorescence

2.2.1 Types of Raman Spectroscopy

Typically standard Raman effect produces very low intensity Raman signal since 1 in 10^8 [25] of the incident light accounts to the Raman signal.

Intensity of the Raman signal is given by the Kramer-Heisenberg-Dirac (KHD) expression written as:

$$I = Kl\alpha^2\omega^4 \tag{2.2.7}$$

where K is a constant, l is laser power, α is polarizability and ω is the frequency of incident light[8]. We can see from the KHD expression above, we can increase the signal by increasing the laser power to a ceratin value taking care not to burn or damage the sample and/or increase the polarizability, discussed in the next section (SERS), or increase the frequency of the incident light. To enhance the Raman signal, there are methods which increases the Raman signal hence making it easy to detect or to study samples of low concentration.

RRS (Resonance Raman Spectroscopy)

While in the standard Raman we excite the molecule to virtual state, in resonance Raman we have to excite the molecules to a higher electronic state as shown in Fig 2.5. This is accomplished by selecting the frequency of the incident light where there will be absorption by the molecules. The molecules that have different absorption bands can be specifically probed at for fewer vibrational modes of complex samples with numerous vibrational modes [4]. This comes with the cost of the possibility of the Raman signal being overwhelmed with the fluorescence signal. To overcome this, one must have to use short wavelegth (deep UV) [1, 26] or use Shifted-frequency incident light and extract the new Raman signal from the unchanged fluorescence signal [21]. This method is reported to have a signal enhancement by a factor of 10^2 to 10^6 [4].

SERS (Surface Enhanced Raman Scattering) Spectroscopy

Surface enhanced Raman spectroscopy uses noble metallic nanostructures of gold, silver or platinum. SERS is base on the substantial enhancement of Raman scattering of molecules adsorbed on these metallic nanostructues. There are two mechanisms of enhancement with combined effects[23]. These are electromagnetic enhancement based on resonance excitation of surface plasmons in the metal and the molecule and molecular enhancement due to the increasing of polarizability of the molecule with enhancement factor of 10^4 to 10^6 in some cases 10^{11} [29, 17].

SERRS (Surface Enhanced Resonance Raman Scattering) Spectroscopy

Surface Enhanced Resonance Raman Scattering Spectroscopy is a combination of enhancement effect of RRS and SERS described above. This method employs the both the advantage of RRS and SRRS to a higher enhancement compared to either of both methods. Enhancement factor can reach 10^{13} to 10^{15} [20].

TERS (Tip Enhanced Raman Scattering) Spectroscopy

Tip Enhanced Raman Scattering Spectroscopy is used as Scanning Probe Microscopy (SPM) Scanning Tunneling Microscopy (STM) or Shear Force Microscopy (SFM) with the ability of simultaneously measure topography by the conventional SPM mode and spectral information from a sample with sub nanometer spatial resolution and high sensitivity [4, 25, 31]. This method focuses the incident light onto a nanometer scale metal-coated (gold or silver) tip of Scanning Probe Microscopy cantilever. The enhancement factor of this method can reach as much as 10^{10} [4, 34].

CARS (Coherent Anti-Stokes Raman Scattering Spectroscopy) Spectroscopy

Coherent Anti-Stokes Raman Scattering Spectroscopy is a 3rd-order nonlinear four-wave optical mixing process in which a picosecond pulsed lasers are used [25, 4]. Here a pump laser of frequency denoted as ω_p and a probe beam of frequency ω_{pr} are mixed with a third beam of frequency ω_S(Stokes frequency) incident on the sample. The frequency difference $\omega_p - \omega_S$ will have to match the frequency of a rotational-vibrational frequency and a resonantly enhanced anti-Stokes signal is generated at a frequency $\omega_{AS} = \omega_p - \omega_S + \omega_{pr}$. [25, 4]. If the frequency of pump beam is the same as that of the probe beam, $\omega_{AS} = 2\omega_p - \omega_S$. This method avoids fluorescence interference and has a signal enhancement factor of 10^4[35].

2.3 Fluorescence Spectroscopy

Fluorescence of materials is described in a simplified diagram called Jablonski diagram as shown in Fig 2.6. There are two kinds of luminescence; fluorescence and phosphorescence. In fluorescence incident light of certain frequencies are absorbed by a material and the molecules are excited to a higher energy singlet states S1, S2 etc. From the diagram, we see that there are different ways for the molecules to be deexcited. One way of deexcitation is via vibrational relaxations (vr) in the singlet state followed be emission or another way is vibrational relaxations followed by internal conversion (ic) or external conversion (ec) followed by vibrational relaxations to the ground state. The other paths of deexatation are internal conversion (ic) from one singlet state to another singlet state followed a process described above. If there is a transition from a singlet state to a triplet state through inter system crossing (isc) followed by emission, it is called phosphorescence[16].

2.3.1 Excitation Spectrum

The shape of the excitation spectrum should be identical to that of the absorption spectrum of the molecule and independent of the wavelengths at which fluorescence is measured as shown in Fig 2.7. In addition, for many organic samples, the strongest (generally the longest) wavelength peak in the excitation spectrum is chosen for excitation of the sample to minimizes possible decomposition caused by the shorter wavelength, higher energy (frequency) radiation.

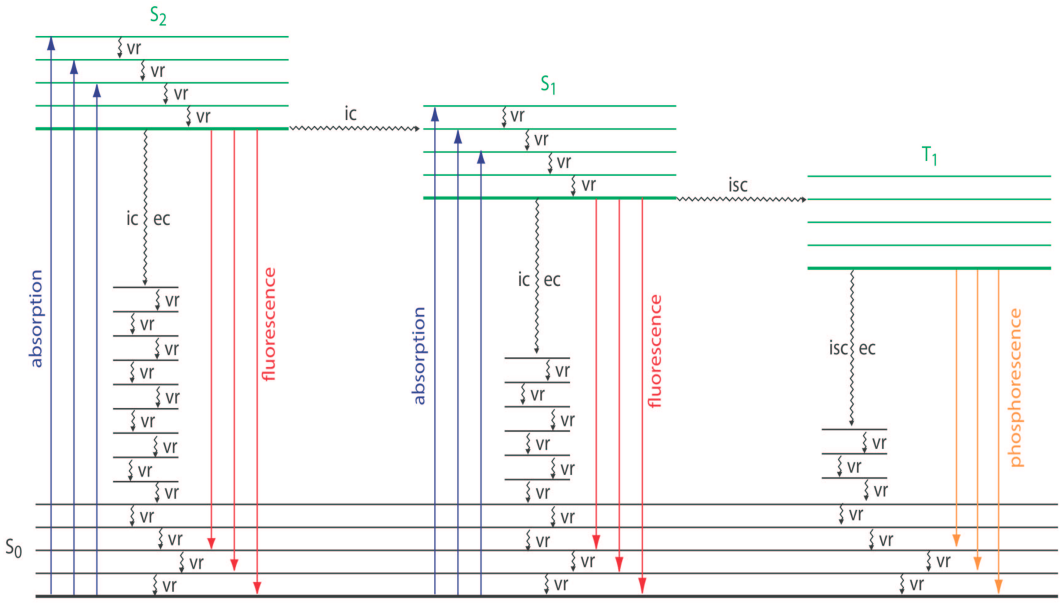

Figure 2.6: Jablonski diagram for fluorescence

2.3.2 Emission Spectrum

The emission spectrum of a compound which results from the radiation absorbed by the molecule. Another property of fluorescence is the the same fluorescence emission spectra is observed irrespective of the excitation wavelength. This is known as Kasha's rule[15].

The emission spectrum is the relative intensity of radiation emitted at various wavelengths. In theory, the quantum efficiency and the shape of the emission spectrum are independent of the wavelength of the excitation radiation. In practice, this is not the case[16]. It has been shown that fluorescence of chlorophyll from a green leaf has a lower short wavelength emission maximum when excited with green light than when excited with blue light. Green light penetrates more deeply into the leaf since it is less absorbed than blue light and the green light excited fluorescence from

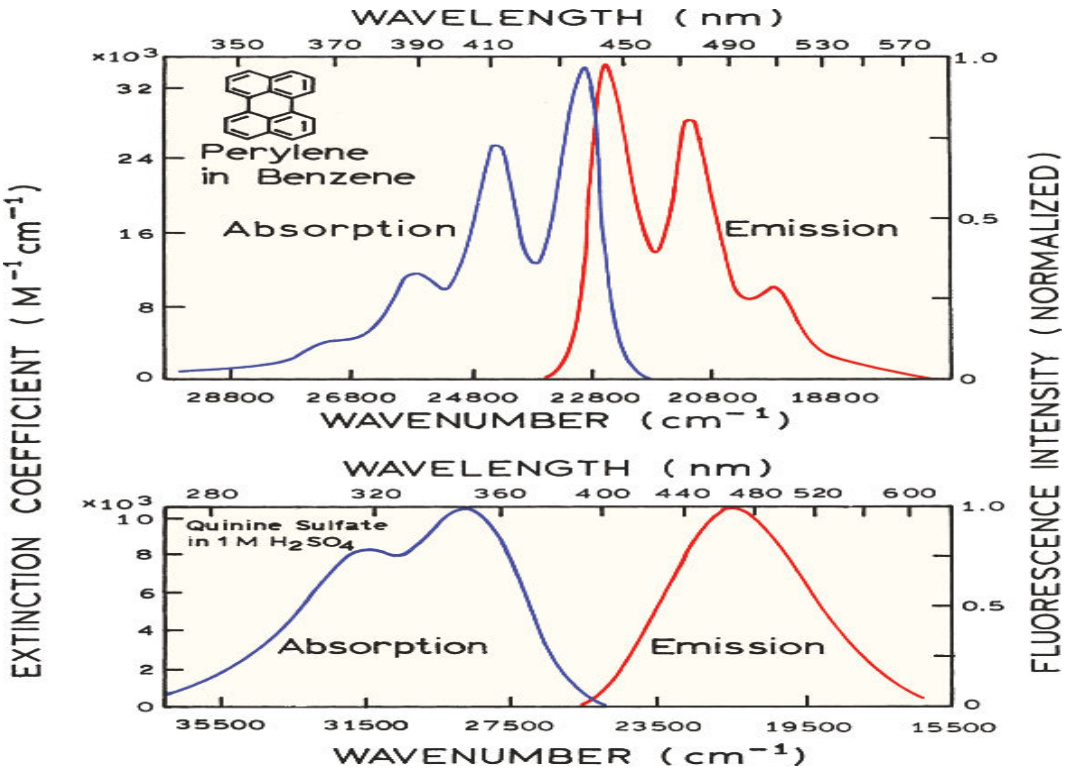

Figure 2.7: Absorption and emission spectra[16]

more inside the leaf is more readily re-absorbed by the chlorophylls on its way to the sample surface. The re-absorption of fluorescence is particularly high in the short wavelength fluorescence where it overlaps with the absorption spectrum of chlorophyll. If the exciting radiation is at wavelength that differs from the wavelength of the absorption peak, less radiant energy will be absorbed and hence less will be emitted.

2.3.3 Stokes Shift

According to the Jablonski diagram Fig.2.6, the energy of emission is lower than that of excitation. This implies that the fluorescence emission occurs at higher wavelengths

than the absorption (excitation). The energy of emission is typically less than that of absorption. Fluorescence typically occurs at lower energies or longer wavelength. The difference between the excitation and emission reciprocal-wavelengths is known as Stokes shift, with unit of cm^{-1} for wavelength in nm.

$$(\frac{1}{\lambda_{ex}} - \frac{1}{\lambda_{em}})10^7 \tag{2.3.1}$$

Chapter 3

Experimental Setup and Procedure

3.1 Experimental setup

One of the main part of this experiment is the nitrogen laser we constructed in the lab. We prepared two types of Nitrogen lasers, TEA(Transversely Excited at Atmospheric pressure) and low pressure type.

3.1.1 TEA Nitrogen Laser

In the TEA type, the laser is constructed using aluminum foils for capacitors, aluminum rods as laser electrodes, write-on transparency sheets as dielectric for the capacitor, small bronze cylinders as spark gap and custom made high voltage power supply. The foil is cut to a size of 45 cm by 47 cm for the common bottom plate of the capacitor and the two plated are cut to 22 cm by 47 cm each to form the top plates of the capacitor. Each capacitor measured to have 67 nF capacitance. The two aluminum rods of length 39 cm and diameter of 1.1 cm each were used as electrodes to for the laser cavity.

To increase the percentage of the nitrogen gas from 78% atmospheric composition, we directed a pure nitrogen gas boiling off from liquid nitrogen dewar directly in to

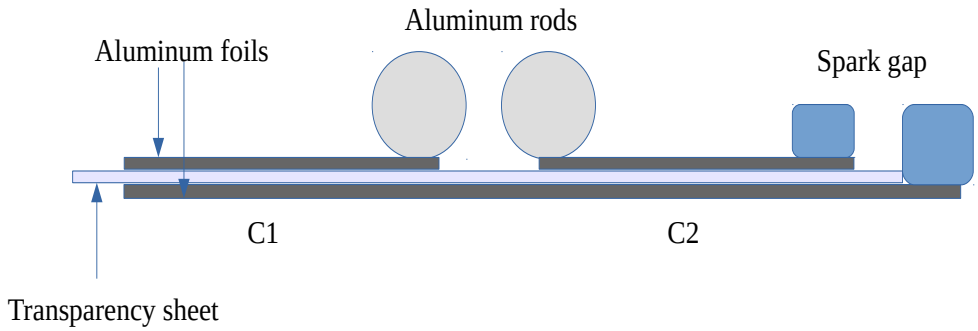

Figure 3.1: Cross section of nitrogen laser

the cavity at the center of the aluminum electrodes.

Figure 3.2: TEA nitrogen laser running with flat electrodes (left) and cylindrical electrodes (right).

3.1.2 Low-pressure Nitrogen Laser

In this part of the setup, we used sealed rectangular ceramic tube containing inside two bronze electrodes separated at 1 cm and having ceramic capacitors rated for 15 KV. The ceramic tube was drilled at two ends and glass tubes were attached with

silicon sealant to form inlet and outlet for the nitrogen gas. The outlet tube was attached to a vacuum pump and the inlet tube was attached to the gas out put tap of the liquid nitrogen dewar. The boil off pure nitrogen gas coming from the dewar was regulated by a ball valve to limit the flow hence controlling and regulating the pressure inside laser cavity. The ball valve is adjusted to a position where the laser power output was visibly maximum when a white paper is placed in the beam path and the threshold power to pump the rhodamine 6G dye is reached.

3.2 Preparation and Nature of the Sample

3.2.1 Raman Spectroscopy

In this experiment we used polystyrene sample which has very low absorbance at 337.1nm [30]. This sample is a polymer of styrene molecules as shown in Fig 3.3. It is prepared from big block by cutting out small rectangular block in such a way that it sit in the sample chamber. Here, one of the main advantage of Raman spectroscopy, no complicated or time consuming sample preparation is needed.

The one critical part of this experiment is to avoid the Rayleigh line while trying to get most of the Raman signals. Since we are not using rejection filter of the laser wavelength the spectrometer is adjusted in a way to avoid detecting the 337.1 nm line. The Raman spectrum of the our polystyrene sample is shown in Fig 4.2

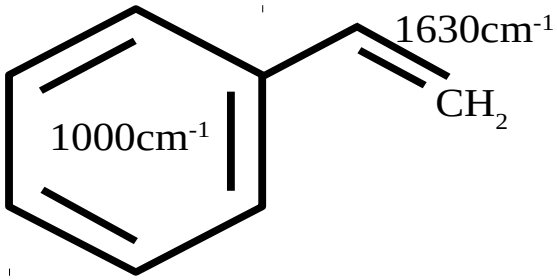

Figure 3.3: Styrene molecule

3.2.2 Fluorescence Spectroscopy

For this part of the experiment, we used niger seed edible oil for fluorescence study. The absorption spectrum of the oil is shown if Fig 3.4. The oils samples are excited

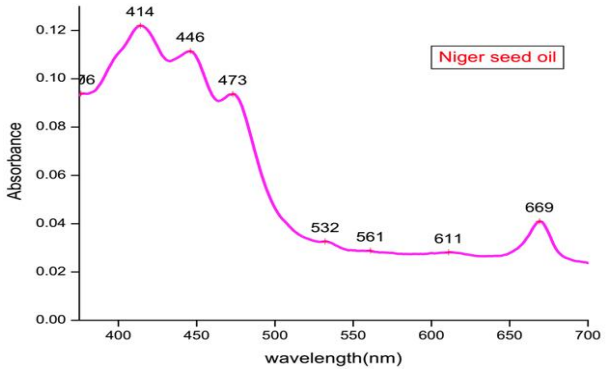

Figure 3.4: Absorption spectrum of niger seed oil

with the dye laser as an excitation source. Even though there is higher absorption in the wavelength range less than 500 nm, we used the dye laser to avoid sample bleaching rather than with the UV laser of 337.1 nm of the nitrogen laser. Fig 3.5 shown the lasing of RG6 while being pumped with the nitrogen laser, coming from the bottom left, and reflected by a mirror to be focused on the cuvette surface holding

the dye by a cylindrical lens (middle left). The cuvette is placed at the middle of the output coupler and the grating forming the dye laser resonator.

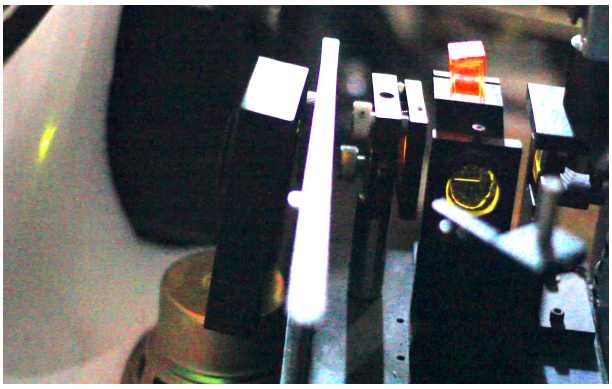

Figure 3.5: Dye laser with RG6

The oil is first heated to 220 ^{0}C for 10 hours in oven and then cooled back down to room temperature. This is to simply simulate the the oil being used in food stuff cooking. Even though when using the oil in a cooking such as frying potato chips there will be another form of contamination far worse. A spectrum of pure unheated oil is measured for reference peak adjustment and then the heated oil is also taken. This is followed by mixing the heated oil with pure oil of different concentration according to the table shown in Table 3.1 and placed in different containers followed by 30 minutes of homogenization by placing the containers in ultrasonic bath.

3.2.3 Instrumentation of Raman Spectroscopy and Fluorescence

The instruments used in this setup according to the schematic shown in Fig 3.6 We have used INSPECTRUM INS-150-252F spectrometer integrated with Hamamatsu temperature controlled CCD sensor cooled to -25 ^{0}C with 1024 by 256 pixel count,

Initial volume(ml)	Added volume(ml)	Total volume(ml)	percentage
4.00	0.25	4.25	05.82
4.00	0.50	4.50	11.11
4.00	0.75	4.75	15.79
4.00	1.00	5.00	20.00
4.00	1.25	5.25	23.81
4.00	1.50	5.50	27.27
4.00	1.75	5.75	30.44
4.00	2.00	6.00	33.33
4.00	2.25	6.25	36.00
4.00	2.50	6.50	38.46
4.00	2.75	6.75	40.74
4.00	3.00	7.00	42.86
4.00	3.25	7.25	44.83
4.00	3.50	7.50	46.67
4.00	3.75	7.75	48.39
4.00	4.00	8.00	50.00

Table 3.1: Sample preparation table for mixing pure and heated oil

made by Acton Research. The spectrum is collected by the SpectraSense software that came with the instrument. Inside the spectrometer, a grating of groove density 1800l/mm blazed at 500 nm is installed. It has a sample chamber attached to the spectrometer with ports at each wall of the chamber. In the chamber there are two lenses one to focus the incoming light on to the sample and another one to collect the light coming form the sample on to the entrance slit of the spectrometer. We have used the side port on the so that we can use it as fluorescence and Raman spectrometer in 90 degree configuration.

3.3 Experimental Setup of Raman spectroscopy

The sample is irradiated with the 337.1 nm wavelength of the nitrogen laser at angle of 45 degrees and the scattered light is collected at 90 degrees from the incoming light.

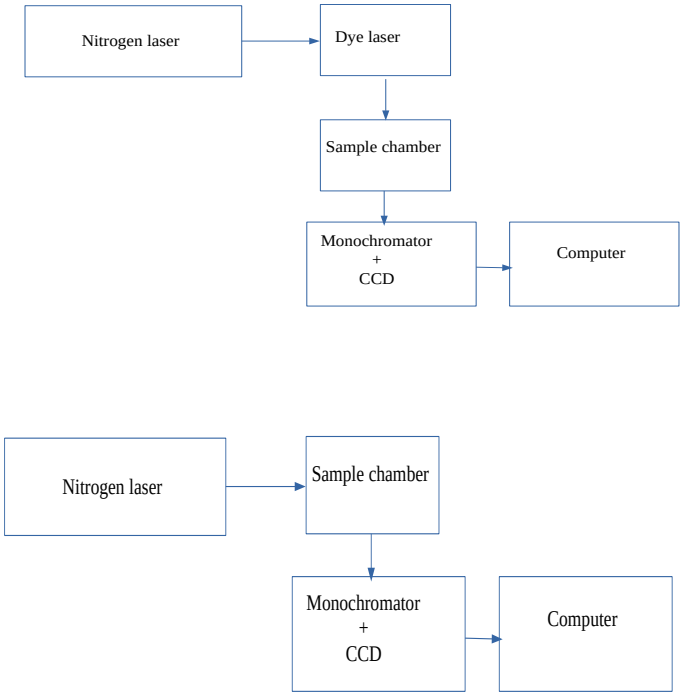

Figure 3.6: Schematic setup of fluorescence spectroscopy(top) and Raman spectroscopy(bottom).

It is then collected by a lens and focused on the entrance slit of the spectrometer. The spectrometer is adjusted to receive the Raman signal by adjusting the grating position in a way that the laser light is not detected by the CCD.

3.4 Measurement and Procedure

Measurement for both Raman and fluorescence spectroscopy is done after calibration of the spectrometer by mercury and sodium vapor lamp. The emission lines of the mercury at 546.07 nm, 576.95 nm and 579.04 nm with emission lines of the sodium vapor lamp at 589.00 nm and 589.59 nm are recorded with the spectrometer. The graph is shown in Fig 3.8 and the linearity is checked by a linear fit as shown in

Fig 3.9. We can see that the second order term is in the order of 10^{-6} showing the linearity of wavelength versus pixel position.

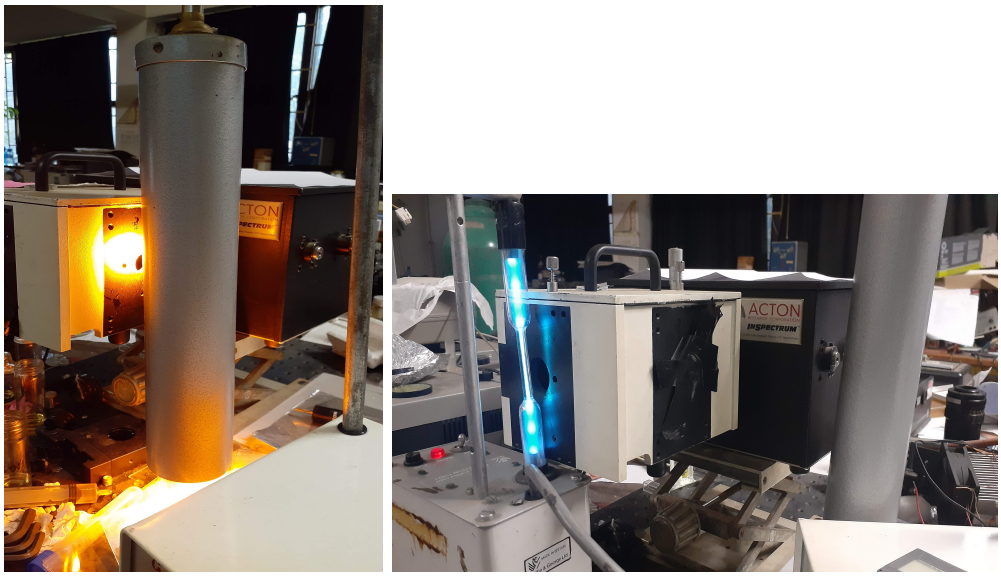

Figure 3.7: Set up of sodium (left) and mercury (right) vapor lamps for calibration of the spectrometer

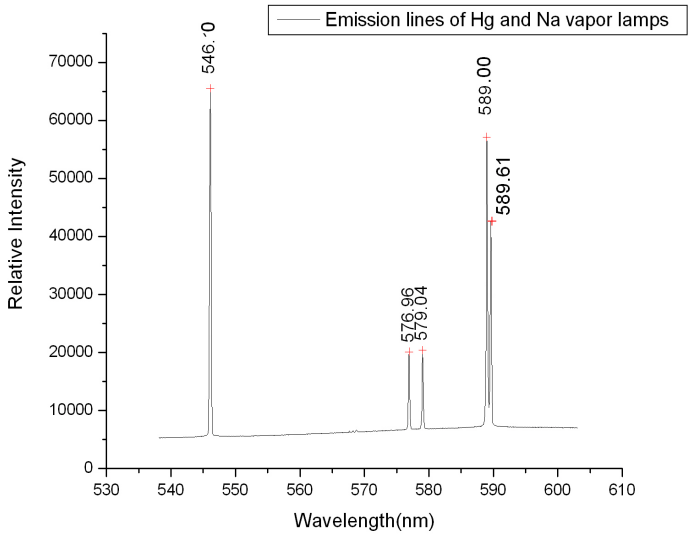

Figure 3.8: Emission lines of mercury and sodium atoms

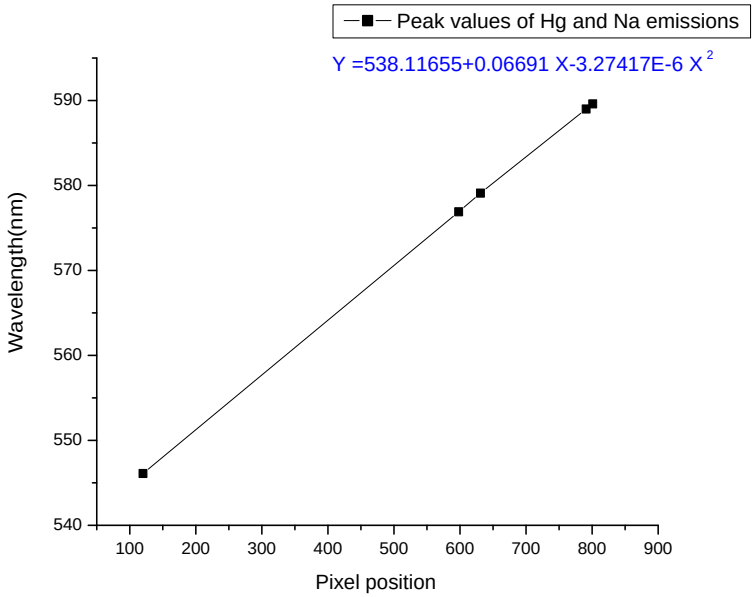

Figure 3.9: Linear fit of wavelength Vs. pixel position for the emission lines of mercury and sodium atoms

Chapter 4

Results, Analysis and Discussion

4.1 Nitrogen laser

The lasers constructed here in this work produced a beam of ultraviolet light of wavelength 337.1 nm as shown in Fig 4.1. After the center wavelength of the spectrometer was set to this wavelength, the signature spectrum that we got can be seen that it is indeed the laser emission of nitrogen lasers. The peak power measured from the Blumlein type construction was 45 KW. while the peak power out put from the low-pressure type was 65 KW. A pulse repetition rate of the TEA lasers was about 15 Hz while for the low- pressure one it was 6 Hz. It was also observed that the TEA lasers have much less divergence which is observed on a plain white paper at close and far distance. This can be explained by the fact that the length of the TEA type laser was about double compared to the low-pressure type.

From this point on, the rest of the experiment was conducted with the low-pressure type because of the higher power output and beam size of 1 cm width which is more suitable to pump the dye laser. Low-pressure lasers of this type are also more efficient and not prone to dielectric break down. The placement of a reflective first-surface mirror at one end of the ceramic tube also helped in producing more power.

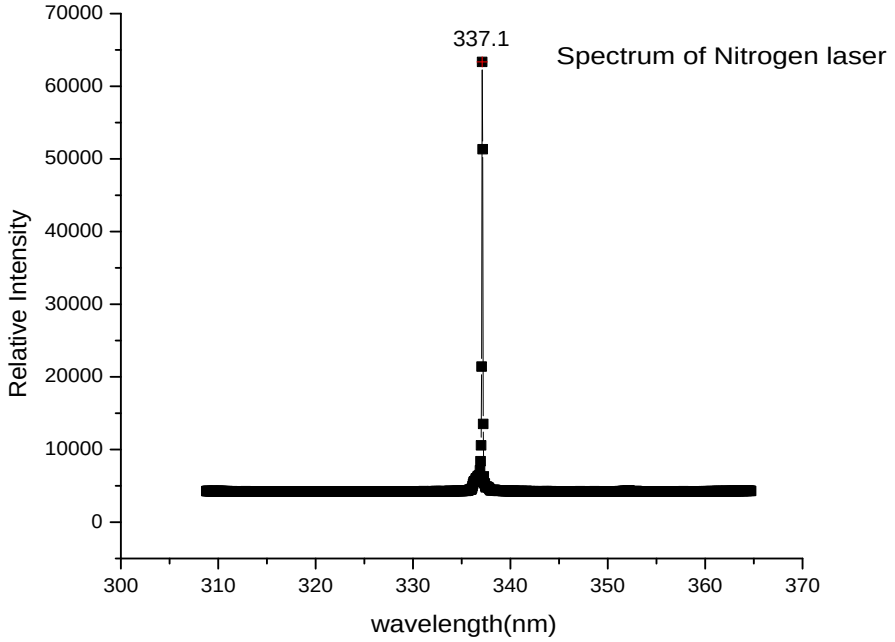

Figure 4.1: Spectrum of nitrogen laser emission

4.2 Raman Spectroscopy

The polystyrene sample under investigation for Raman analysis gave a very close result with the reference Raman spectrum. The result shown in Fig 4.2 is compared with the reference spectrum in Fig 4.3.

The two main peaks, one near 1000 cm^{-1} due to the breathing mode of the benzene ring, is dominant in this spectrum while the vinyl bond stretch in styrene molecule near 1630 cm^{-1} with decrease in intensity as this molecule polymerizes to form the long chain polymer so called polystyrene. Both in this work and the reference sample, this peak position is shifted to 1564 cm^{-1} and 1602 cm^{-1} respectively. Raman peaks at the 620.9 cm^{-1} and 795.8 cm^{-1} are not visible in this work since we adjusted the spectrometer to avoid the laser frequency and since the two peaks are very close to the

Sample	Reference	Deviation	Percentage error
1001.97	1001.4	-0.43	0.04
1041.35	1031.8	9.55	0.93
1564.79	1602.3	-37.51	2.34
2584.35	2852.4	-268.05	9.40
2901.44	2904.5	-3.06	0.11
3111.31	3054.3	57.01	1.87

Table 4.1: Comparison table of the Raman peaks of our sample with reference peaks

laser, we have to avoid them to prevent the CCD from being saturated and become unable to detect the Raman signals above 1000 cm^{-1}. This can be overcome if we could use Rayleigh rejection filter, not available in our laboratory at the moment, that will filter out only the laser and transmit the Raman signals.

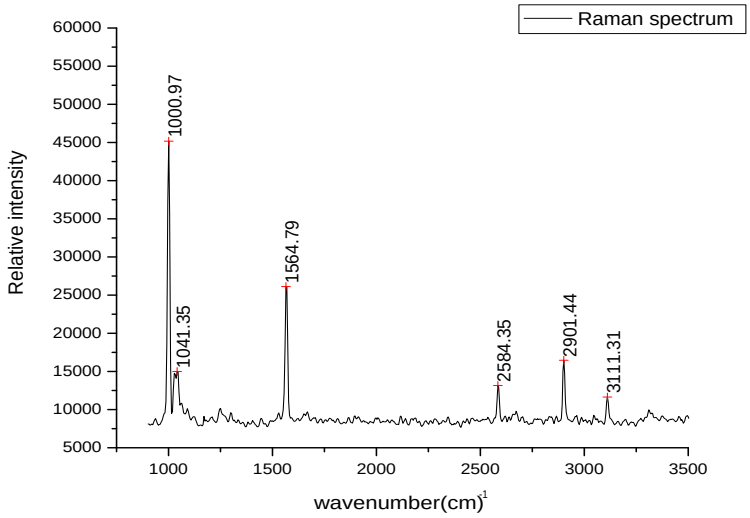

Figure 4.2: Raman spectrum of Polystyrene sample

4.3 Fluorescence Spectroscopy

In this part of the experiment we can see from Fig 4.4 that the peak emission of the oil at 675 nm decreases with increasing of adulteration. This is in agreement with the

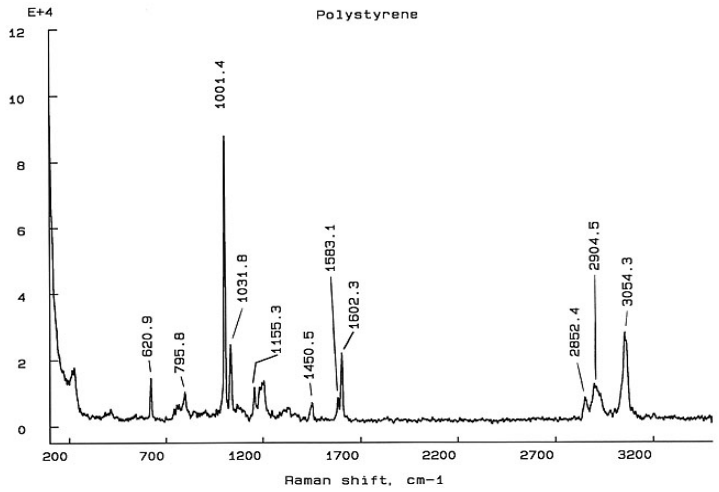

Figure 4.3: Reference Raman spectrum of Polystyrene sample

work of HAO *et al.*[12] in which they show a decrease in intensity with increasing of adulteration from 5% to 50 %. This fluorescence peak is associated with the presence of chlorophyll in the oil[12]. In our work, there is also a shift in peak value of the emission for the pure heated oil sample to a lower wavelength. This can be explained by the newly formed fluorophores and other complex chemicals[19] created by the heating of the oil using another instrument such as gas chromatography[9, 14]. The graphs plotted in Fig 4.4 are the results of different concentration of the niger seed oil prepared according to Table 3.1 and the fluorescence of each sample is plotted individually and later combined to show the final result we see on the graph. The graph in Fig 4.5 shows the linear fit of the peak value with respect to the percentage of adulteration of the oil. There is a linear relationship between the increase of concentration of adulteration with a decrease of fluorescence intensity. This can be useful in identification of an oil sample that is mixed with previously used oil is mixed with pure oil. Even if food particles are filtered out of the used oil to make it clear

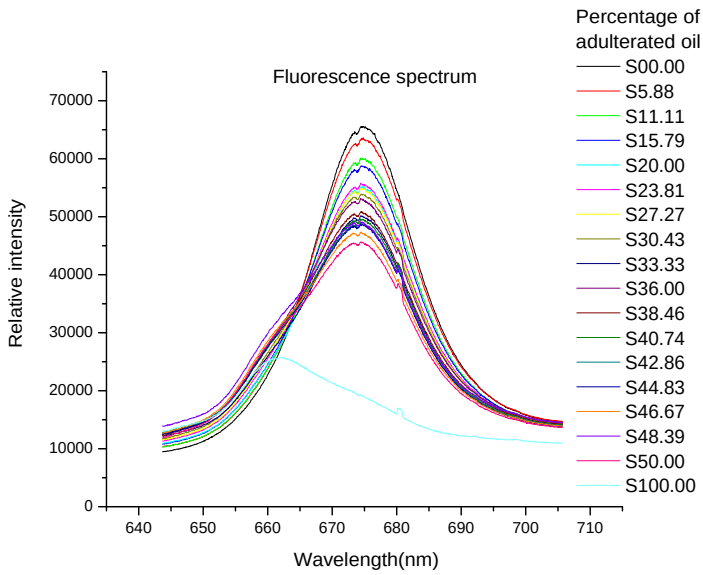

Figure 4.4: Intensity Vs. wavelength for different percentage of adulteration

enough to be mixed with pure oil, this method can detect adulteration by simply comparing the fluorescence spectra of the samples.

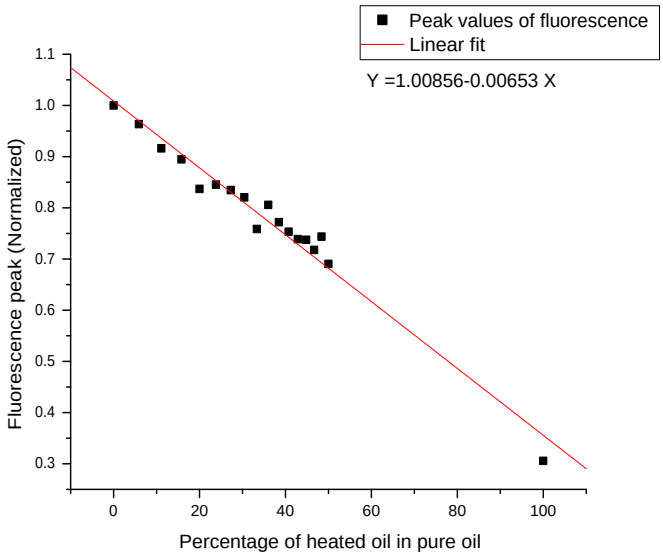

Figure 4.5: Peak intensity Vs. percentage of adulteration

Chapter 5

Conclusion and Recommendations

5.1 Conclusion

5.1.1 Nitrogen Laser

This work shows very satisfying results of the construction of the nitrogen laser and the collection of Raman spectrum of polystyrene sample and a reliable result of showing contamination or adulteration of edible niger seed oil. With most simple method of laser construction and availability of most of the instruments used in this work, we are satisfied with the results we accomplished. The construction and performance of the laser was successful. In addition to delivering the laser output, we also used it as pump source for the Raman and laser induced fluorescence experiments we conducted in this work.

5.1.2 Raman Spectroscopy

The experiment regarding the Raman spectroscopy resulted in an acceptable Raman spectrum of the polystyrene sample under test. Though it is not comparable with modern Raman spectrometers, it is very good result considering the simplicity of our setup consisting the bare minimum of components used for this kind of experiment.

We accomplished this with the combination of effects that were in our favor by the fact that the choice of the sample that doesn't have an absorbance at the nitrogen laser line of 337.1 nm thus not producing fluorescence signal which can overwhelm the Raman signal, and the high groove density 1800l/mm of the grating in the spectrometer.

5.1.3 Fluorescence Spectroscopy

In the fluorescence study of the niger seed oil, we have seen that it is very reliable setup. Compared to the Raman spectroscopy setup, it is easier and simpler to run. We managed to get a good result in terms of detecting contamination of the edible oil. We have achieved a detection limit of 1.61% contamination as can be seen from the Table 3.1. This limit value can be lowered more by increasing the integration time of the spectrometer so that the difference in the intensities between two fluorescence spectrum of the oils can be maximized.

5.2 Recommendations

5.2.1 Nitrogen Laser

The current build of the laser is the bare minimum of what can be done with nitrogen laser in this lab. The power supply part of the setup can be scaled up by using custom coil winding of the secondary winding of the flyback transformer with thicker coil for a higher wattage, or by using ready made ZVS(Zero voltage switching) driver circuit available on sale for very cheap price. Also the availability of cheap ceramic capacitors rated for higher voltage, up to 40 KV and 1000pF capacitance rating with

longer cavity length(up to 1 meter), we can produce a couple of Mega watts level pulse out of this kind of laser at high repetition rate. This will in turn can lead to higher output of dye lasers for further studies such as Resonance Raman, Coherent Anti-Stokes Raman and LIBS (Laser-Induced Breakdown Spectroscopy).

5.2.2 Raman Spectroscopy

The Raman experiment can also use higher power of this laser. With combination of monochromators for the laser and the Raman signal, we can have resonance Raman effect which is more easy to see the Raman signal without long acquisition time. this laser.

Another issue with the dispersive type Raman spectroscopy is the small amount of the signal that passes through the entrance slit and detected by the CCD. This can be overcome by the now industry standard FT-Raman. We propose building FT-Raman instrument in this lab by using easy to get components and filter assemblies using old or out-of-use FTIR instruments that are available in our campus. In addition to up cycling these instruments, it can be used by students for further studies rather than buying a new and expensive instrument which have only one wavelength 785 nm of 1064nm. But we can make this as flexible as we want in our proposed setup.

5.2.3 Fluorescence Spectroscopy

With regard to the fluorescence spectroscopy, we didn't counter any major problem in this work. But most fluorescence spectroscopy is done with monochromators that are capable of tuning the wavelength which is not the case in our type of monochromator. A computer controlled one would make future works easier.

Bibliography

[1] Asher S. A, *"UV resonance Raman studies of molecular structure and dynamics: application in physical and biophysical chemistry"*, Annual Review of Physical Chemistry (1998).

[2] V. Aboites A. Vazquez, *High-Efficiency Low-Pressure Nitrogen Laser*, IEEE Journal of Quantum Electronics **29** (1993), no. 8, 2364–2370.

[3] A. W. Ali, A. C. Kolb, and A. D. Anderson, *Theory of the Pulsed Molecular Nitrogen Laser*, vol. 6, OSA, Dec 1967.

[4] Koya S.K. Huang C. et al. Auner, G.W., *Applications of Raman spectroscopy in cancer diagnosis*, (2018).

[5] J. B. de Oliveira e Souza B. Oliveira dos Santos and C. A. Massone, *A 3 Percent Efficiency N2 laser*, Appl. Phys. Lett. B **41** (1986), 241–244.

[6] W. R. Bennett, *Inversion Mechanisms in Gas Lasers*, Appl. Opt. **4** (1965), no. S1, 3–22.

[7] B. Steyer D. Basting, F. P. Schäffe, *A simple, high power nitrogen laser*, Opto-electronics **4** (1972), 43–44.

[8] Geoffrey Dent Ewen Smith, *Modern Raman Spectroscopy–A practical approach*, John Willey and Sons.

[9] J. M. Herrero-Martinez F. Troya, M. J. Lerma-Garcia and E. F. Simo-Alfonso, *Classification of vegetable oils according to their botanicalorigin using n-alkane profiles established by GC-MS*, Food Chem. **167**, 36–39.

[10] E. T. Gerry, *Pulsed-Molecular-Nitrogen Laser Theory*, vol. 7, 1965.

[11] Bruno Godard, *A simple high-power large-efficiency N2 ultraviolet laser*, IEEE Journal of Quantum Electronics **10** (1974), no. 2, 147–153.

[12] Shiguo Hao, Lian Zhu, Ronglong Sui, Mengling Zuo, Ningning Luo, Jiulin Shi, Weiwei Zhang, Xingdao He, and Zhongping Chen, *Identification and quantification of vegetable oil adulteration with waste frying oil by laser-induced fluorescence spectroscopy*, OSA Continuum **2** (2019), no. 4, 1148–1154.

[13] H. G. Heard, *Ultra-violet Gas Laser at Room Temperature*, Nature, November 16, 1963 667.

[14] Long Deng Ya-Wei Fan Hongyan Li Jing Li Ze-Yuan Deng Jun Cao, Xian-Guo Zou, *Analysis of nonpolar lipophilic aldehydes/ketones in oxidezed edible oils using HPLC-QqQ-MS for the evaluation of their parent fatty acids*, Food Research International **64** (2014), 901–907.

[15] M. Kasha, *Characterization of electronic transitions in complex molecules*, Disc. Faraday **9**, 14–19.

[16] Joseph R. Lakowicz, *Principles of Fluorescence Spectroscopy. Third edition*, Springer, 2010.

[17] E. C. Le Ru, E. Blackie, M. Meyer, and P. G. Etchegoin, *Surface enhanced Raman scattering enhancement factors: A comprehensive study*, The Journal of Physical Chemistry C **111** (2007), no. 37, 13794–13803.

[18] Donald A. Leonard, *Saturation of the molecular nitrogen second positive laser transition*, AIP, 1965.

[19] Patricia S. Uriarte Maria D. Guillén, *Aldehydes contained in edible oils of very different nature after prolonged heating at frying temperatures: Presence of toxic oxgenated α,β unsaturated aldehydes*, Food Chemistry **131** (2012), 915–926.

[20] Graeme McNay, David Eustace, W. Ewen Smith, Karen Faulds, and Duncan Graham, *Surface-Enhanced Raman Scattering (SERS) and Surface-Enhanced Resonance Raman Scattering (SERRS): A Review of Applications*, Appl. Spectrosc. **65** (2011), no. 8, 825–837.

[21] Andrew Riches-C. Simon Herrington Michael Mazilu, Ana Chiara De Luca and Kishan Dholakia, *Optimal algorithm for fluorescence suppression of modulated Raman spectroscopy*, OPTICS EXPRESS **18** (2010), no. 11.

[22] B. S. Patel, *Compact high-power TEA N2 laser*, Review of Scientific Instrumnets **49** (1978), 1361–1363.

[23] Marek Procházka, *Surface-enhanced Raman spectroscopy bioanalytical, biomolecular and medical applications*, Springer, 2016.

[24] S. M. Curry R. Cubeddu, *A Simple High-Power Pulsed Nitrogen Laser*, IEEE Journal of Quantum Electronics **29** (1973), no. 8, 499–500.

[25] Liwu Zhang Daniel Wolverson K. Valev R. Jones, David C. Hooper, *Raman Techniques: Fundamentals and Frontiers*, Nanoscale Research Letters **14:231** (2019), 1–34.

[26] Moskevets E Dey P Dey BK Lednev IK. Ralbosky NM, Egorov V, *Deep-Ultraviolet Raman Spectroscopy for cance diagnosis: A feasibility study with cell lines and tissues*, Cancer stud. Mol. Med. Open J. **5(1)** (2019), 1–10.

[27] Chandrasekhara Venkata Raman, *A new radiation*, Indian Association for the Cultivation of Science (1928).

[28] John D. Shipmann, *Travelling wave excitation of high power gas lasers*, Appl. Phys. Lett. **10** (1967), no. 1, 147–153.

[29] Daniel O. Sigle, Elaine Perkins, Jeremy J. Baumberg, and Sumeet Mahajan, *Reproducible Deep-UV SERRS on Aluminum Nanovoids*, The Journal of Physical Chemistry Letters **4** (2013), no. 9, 1449–1452, PMID: 26282297.

[30] Chunlin Zhou Tong Li and Ming Jiang, *UV absorption spectra of polystyrene*, Polymer Bulletin **25** (1991), 211–216.

[31] P. Verama, *Tip-enhanced Raman spectroscopy: technique and recent advances.*, Chem. Rev. **117**.

[32] KH Wagner, *Über das nachleuchten von A, N2 and N2 plus CH4 nach stoßanregung durch elektronenlawinen*, vol. 19, De Gruyter, 1964.

[33] A. Nomura Y. Saito and T. Kano, *Energy enhancement and volume effect between parallel and transverse gas flow N2 laser*, Journal of Applied Physics **63** (1988), 2526–2528.

[34] Zhenglong Zhang, Shaoxiang Sheng, Rongming Wang, and Mengtao Sun, *Tip-enhanced Raman spectroscopy*, Analytical Chemistry **88** (2016), no. 19, 9328–9346, PMID: 27571253.

[35] M. Zumbusch, A. Müller, *Coherent anti-Stokes Raman Scattering Microscopy*, Chemphyschem : a European journal of chemical physics and physical chemistry **8(15):2156-70** (2007).